Selective electrocatalytic hydrogenation of α,β-unsaturated ketone on (111)-oriented Pd and Pt electrodes

Villalba, M.A.; Koper, M.T.M.

Electrochimica Acta 417 (2022) 140264

Contents lists available at ScienceDirect

Electrochimica Acta

journal homepage: www.journals.elsevier.com/electrochimica-acta

Selective electrocatalytic hydrogenation of α,β-unsaturated ketone on (111)-oriented Pd and Pt electrodes

Matias A. Villalba, Marc T.M. Koper *

Leiden Institute of Chemistry, Leiden University, PO Box 9502, Leiden, 2300 RA, The Netherlands

ARTICLE INFO

Keywords:
Hydrogenation
Electrocatalysts
(111) facet
Dissociative adsorption
CO-poisoning
Hydrogen co-adsorbed

ABSTRACT

In this paper, we study the electrocatalytic reduction of methyl vinyl ketone on Pt(111) and Pd-modified Pt(111) electrodes, as well as some of its expected hydrogenation derivatives and isolated functional moieties. The selectivity and Faraday efficiency have been calculated via sampling the catholyte solution after two hours of electrolysis. Furthermore, the adsorbates involved in the deactivation process on both surfaces were studied by means of potential opening experiments and in situ infrared spectroscopy. The Pd-modified Pt(111) electrode is very active (even mass transport limited) for the selective electrochemical hydrogenation of the C=C to 2-butanone, in the hydrogen underpotential deposition potential window (between 0 and 0.2 V_{RHE}), with limited poisoning. Pt(111) is much less active, and poisons rapidly with adsorbed CO. The poison is formed from the C=C bond, not from the C=O moiety, as evidenced by the same poisoning occurring for ethylene. Further hydrogenation to the saturated alcohol happens at more negative potentials, but with 2-butenol as intermediate, not 2-butanone, as the latter species interacts too weakly with the (111) surface.

1. Introduction

Selective hydrogenation is a key reaction in catalytic chemistry because it is one of the most important processes towards upgrading biobased sources to chemical intermediates. Obtaining high selectivity remains one of the main challenges of current catalytic methods [1]. Electrocatalytic Hydrogenation (ECH) could offer advantages because a) it is a clean procedure using renewable electricity (electrons are the reducing agent), b) in addition to the catalyst, also the potential can be tuned to hopefully benefit selectivity, and c) it may involve full utilization of (renewable) energy by pairing two different reactions on both the anode and the cathode [2].

It is well known that the hydrogenation of the C=C bond is thermodynamically preferred over hydrogenation of the C=O bond [3]. However, chemoselectivity is more unpredictable when both carbonyl and vinyl groups are present in a single molecule, such as in α,β-unsaturated ketones and aldehydes. A review by Murzin et al. summarized the extensive experimental results regarding heterogeneous catalysts and structure of the organic reagent [4]. More recently, it has been demonstrated, using computational tools, that steric effects are one of the most important factors in governing selectivity [5]. For example, adding more bulky groups adjacent to C=C in the unsaturated aldehyde lowers the total selectivity towards production of alkyl aldehydes [6]. Another related property is the preferred adsorption mode of the reactant, which has been addressed computationally for simple unsaturated molecules on different Pt and Pd surfaces [7]. Especially for unsaturated aldehydes, the Pt(111) surface strengthens the di-$\sigma_{C\text{-}C}$ interaction compared to ethylene (-17.8 vs -15.3 kcal/mol, respectively), with the C=O dangling free. On Pd(111), a new mode involving coplanar adsorption of $\pi_{C\text{-}C}$ and $\pi_{C\text{-}O}$ gives a major stabilization effect (-39 kcal/mol) and is therefore the proposed configuration. Experimental results obtained under UHV conditions showed the high selectivity for acrolein hydrogenation to propylene on Pt(111) via η2-trans adsorbed species [8], while propenol is the main product on the Pd(111) surface, via an oxopropyl intermediate [9]. In aqueous solution, crotonaldehyde is fully hydrogenated to its corresponding saturated ketone on a Pd/C catalyst, whereas on a Pt/C catalyst 85% of butanal is obtained plus 10% and 5% of the unsaturated and saturated alcohol, respectively [10].

There is extensive literature on the ECH of individual unsaturated bonds (vinyl [11], carbonyl [12] or even aryl [13]). As for the electrocatalyst, Pt group elements have been extensively utilized for ECH of carbonyl groups [14] (primarily in ketones and aldehydes) and hydrogenation of C-C double bonds [11,15] at potentials above 0 V vs RHE. However, it is still unclear which double bond will be reduced first, or in

* Corresponding author.
E-mail address: m.koper@chem.leidenuniv.nl (M.T.M. Koper).

https://doi.org/10.1016/j.electacta.2022.140264
Received 10 December 2021; Received in revised form 18 February 2022; Accepted 21 March 2022
Available online 25 March 2022

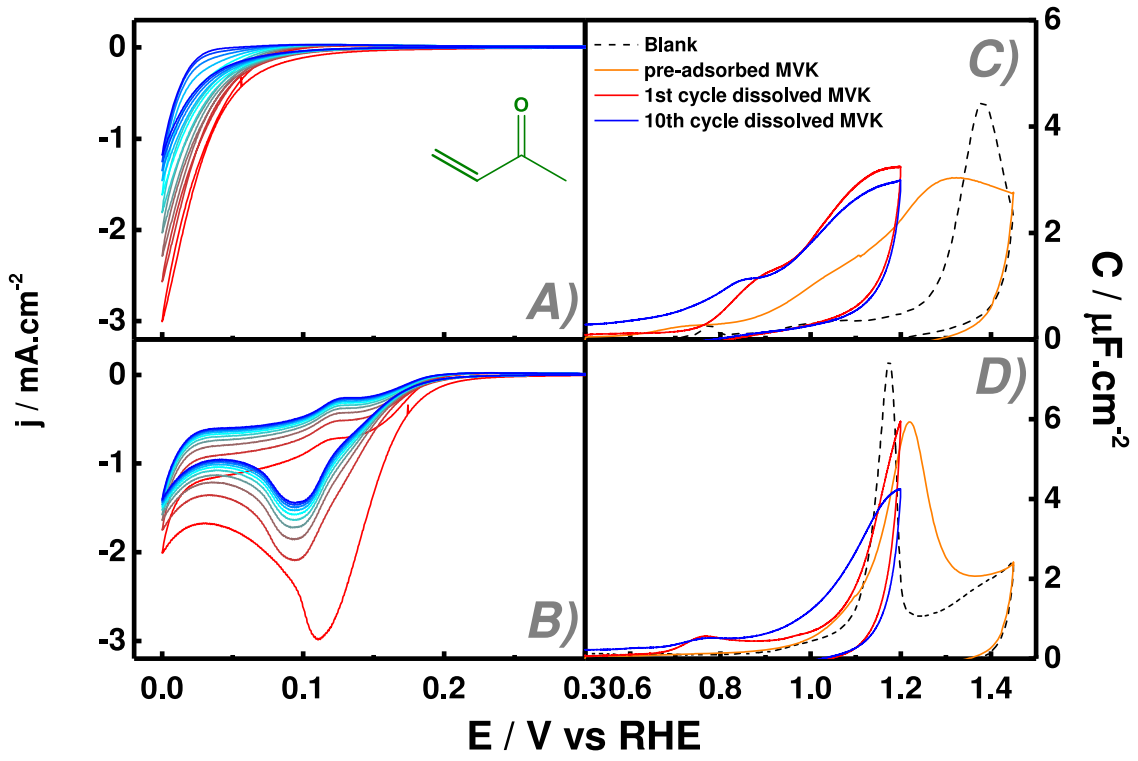

Fig. 1. Consecutive cyclic voltammetry of 10 mM MVK in 0.1M sulfuric acid solution for A) Pt(111) and B) PdML-Pt(111) electrodes at 50 mV s^{-1} starting from and ending at E_{ads}= 0.5 V. 1st and the 10th cycle (red and blue lines, respectively) at 50 mV s^{-1}, and anodic scan at 10mV s^{-1} of dissolved and pre-adsorbed MVK at E_{ads}= 0.5 V (orange lines) for C) Pt(111) and D) PdML-Pt(111) electrodes. The black dashed line is the blank CV at 10 mV s^{-1}.

which sequence they are reduced, when both unsaturated functional groups are present in the same molecule. It has been observed that the vinyl group requires a lower cathodic potential for its reduction than the carbonyl moiety [16]. An example of this preference is the reduction of crotonaldehyde on a Cu electrode [17], which has butanal as the most abundant reaction product at -0.2 V vs. RHE.

Besides the electrode material, the product distribution can be altered by changing the potential and the atomic structure of the catalyst. For instance, Shimazu and Kita observed that if the potential of the bulk electrolysis is made more negative, the selectivity of the ECH of 1,3-butendiene on a Pd foil or film electrode shifts from 55% of 1-butene (partially hydrogenated product) to ca. 70% of butane (fully hydrogenated product) [18]. The crystallographic structure also plays an important role on the adsorption mode (e.g. ethyl pyruvate [19] and methane [20]) and hence on the selectivity.

In this work, we use Pt and Pd-monolayer-modified Pt single-crystal (111) electrodes to evaluate the reactivity and selectivity of the electrochemical hydrogenation of vinyl methyl ketone, an α,β-unsaturated ketone. The isolated moieties (primarily ethylene) are also reduced to study their hydrogenation potential window, their dissociation leading to poisoning species, and to propose potential reaction pathways. Our results will contribute to the aim of selective ECH of complex organic molecules, by improving our mechanistic understanding of the pathways involved.

2. Material and methods

All solutions were prepared using ultrapure water (MilliQ gradient, ≥18.2 MΩcm, TOC < 5 ppb) containing suprapur sulfuric or perchloric acid, 96 and 70% respectively, as supporting electrolyte (Sigma Aldrich). The palladium precursor employed for the electrodeposition was $PdSO_4$ 98% (Sigma Aldrich). The organic substrates 1-buten-2-one (methyl vinyl ketone, MVK), 1-buten-3-ol, 2-butanone, 3-butanol were 90% (with 0.3-1.0% hydroquinone as stabilizer), 97%, >99% and 99.5%, respectively, all provided by Sigma Aldrich. The ethylene employed was grade 4.5 supplied by Air Liquide.

The platinum single crystals were flame annealed before each experiment. They were either a 3 mm bead for the voltammetric experiments or a 1 cm disk for the bulk electrolysis and spectroelectrochemical experiments. A palladium monolayer was electrodeposited on Pt(111) followed a previously reported procedure [21]. Briefly, the potential was cycled between 0.9 to 0.06V in a solution containing 1.10^{-4} M of $PdSO_4$ for ca. 15 cycles with a scan rate of 50 mV s^{-1}.

All the experiments were conducted after purging the solution and the headspace of the cell with Ar for at least 20 minutes, except when the organic reagent was gaseous (ethylene). All the potentials were measured and referred to the Reversible Hydrogen Electrode (RHE), and a platinum mesh was used as counter electrode. To ensure the cleanliness of the glassware and Teflon o-rings/septa, all the materials were kept in permanganate solution overnight, rinsed with an acidic solution of diluted hydrogen peroxide and finally boiled five times in MilliQ water.

The voltammetric studies were performed in a conventional three-electrode cell with the single-crystal working electrode in hanging meniscus configuration. For static electrode experiments, an Autolab PGSTAT12 potentiostat was used to control the potential, and the solution resistance was compensated via positive feedback technique. A Biologic SP-300 multichannel potentiostat was utilized for experiments under rotating electrode conditions, using impedance spectroscopy for the ohmic resistance determination. The rotation rates were adjusted with a Modulated Speed Rotator from Pine Research Instrumentation and a home-made connector for single crystal electrodes was employed. Electrolysis at constant potential was performed in the hanging meniscus configuration in a two-compartment H-cell separated with a Nafion proton exchange membrane. The sampling procedure was conducted via a septa system without stopping the reaction nor breaking the contact of the electrode with the solution. The reactant and products during bulk electrolysis were analyzed by an HPLC Shimadzu LC-20A

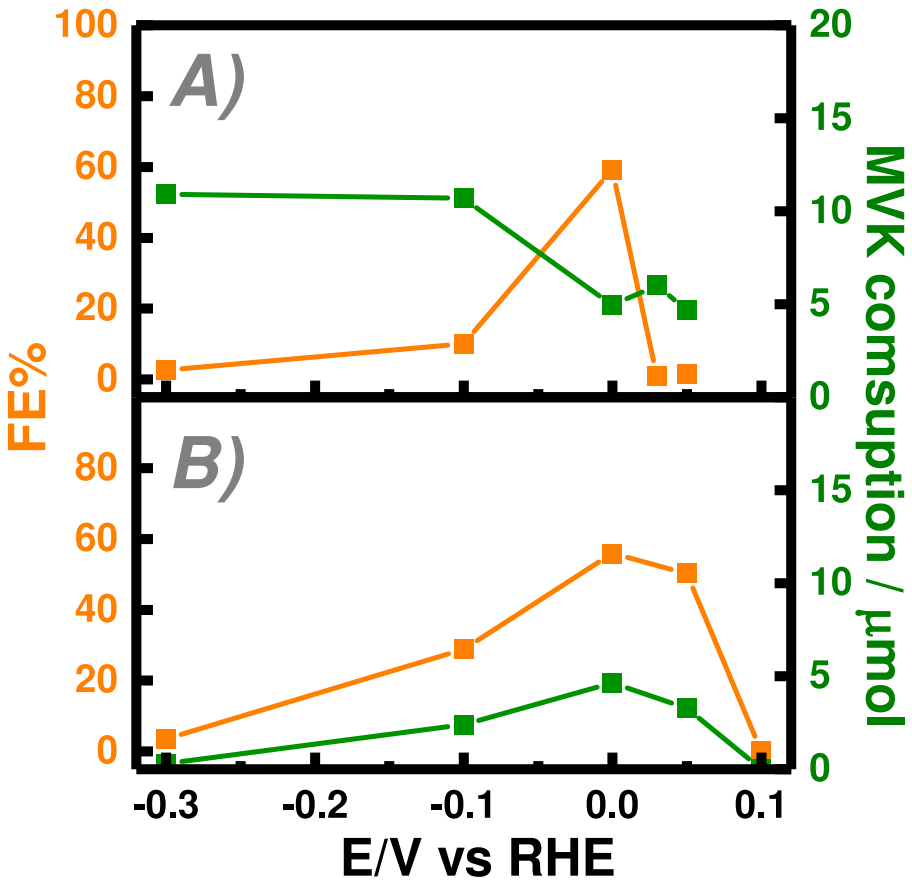

Fig. 2. Faraday Efficiency and reagent consumption after 2 hours of ECH of MVK using A) Pt(111) and B) PdML-Pt(111) electrodes as a function of the applied potential. Main product on both electrodes is 2-butanone.

system with sample volumes of 20 μL, using an Aminex HPX-87H column at 45°C and mobile phase pH-adjusted with sulfuric acid (0.5 mM) solution.

In situ Fourier Transform Infra-Red (FTIR) Spectroscopy experiments used a home-made cell with a Pt foil counter electrode surrounding the working electrode for a homogeneous current distribution. The reference electrode was a self-contained RHE. Ar or ethylene was used to purge the solution and headspace. Experiments were performed with a Bruker Vertex 80v IR spectrophotometer in external reflection configuration using a CaF_2 prism beveled at 60°. The single-crystal electrode was pressed against the optical window creating a thin layer. The experiments were performed with p- or s-polarized light for differentiation of soluble and adsorbed species. The presented spectra correspond to an average of 200 interferograms with 4 cm^{-1} resolution. The spectra in this work are presented as difference spectra between the working potential and a reference potential, controlled by an Autolab PGSTAT101. Therefore, positive bands indicate consumption of solution or adsorbed species, while negative bands indicate generation of species, or a corresponding reorientation of (adsorbed) species.

3. Results and Discussion

A fingerprint of the electrochemical behavior of MVK in acidic media is gained via cyclic voltammetry. Figure 1 shows the voltammetric measurement starting from and ending at the adsorption potential (0.5 V) in presence of 10 mM of MVK for both Pt(111) and PdML-Pt(111) electrodes in panel A and B, respectively. Additionally, the electrooxidation of pre-adsorbed MVK at low scan rate (normalized by scan rate), using the same color notation, is plotted for comparison in panels C and D. The blank CVs are given in Fig. S1 (see Supporting information).

On the Pt(111) electrode, a catalytic reduction current with an onset potential of ca. 0.13 V is observed, the intensity of which decreases upon cycling. This deactivation process is irreversible in the scanned potential window; a stable CV profile is obtained after about 10 cycles (Fig. 1A). By contrast, an apparently mass-transport limited reduction wave with an onset potential of around 0.2 V is observed on PdML-Pt(111) (Fig. 1B). In the first cycle the cathodic current reaches a maximum value of ca. -3 $mA.cm^{-2}$ at 0.11 V while from the second cycle onwards, the peak potential shifts cathodically by 20 mV and the current drops continuously for at least ten cycles and then stabilizes. Two important observations can be extracted from these voltammetric experiments. First, the reduction of the MVK starts at the potential where the hydrogen displaces the adsorbed sulfate on PdML-Pt(111) [22], whilst on Pt(111), MVK reduction is much slower and starts closer to the onset potential for hydrogen evolution. Second, the current density drops drastically on both materials; it almost reaches the values for the blank CV for the Pt(111) electrode, whereas the PdML-Pt(111) electrode retains part of the initial electroactivity (that is, it is more resistant to total deactivation).

Under mass-controlled conditions in a hanging meniscus configuration, using the Hanging Meniscus Rotating Disk (HMRD) technique, the limiting current is attained at $E \leq 0.1V$, coinciding with the potential for the mixed-controlled current using a stagnant electrode. Furthermore, the slope from Koutecky-Levich plot (see Fig. S2 in the Supporting Information) on PdML-Pt(111) gives a diffusion coefficient of 8.07×10^{-7} $cm^2\ s^{-1}$, considering a 2-electron process and the kinematic viscosity of pure water. The calculated value differs by one order of magnitude from the reported diffusion coefficient of acrolein or methyl ethyl ketone (1.2×10^{-5} and 9.8×10^{-6} $cm^2\ s^{-1}$) [23], which suggests that MVK

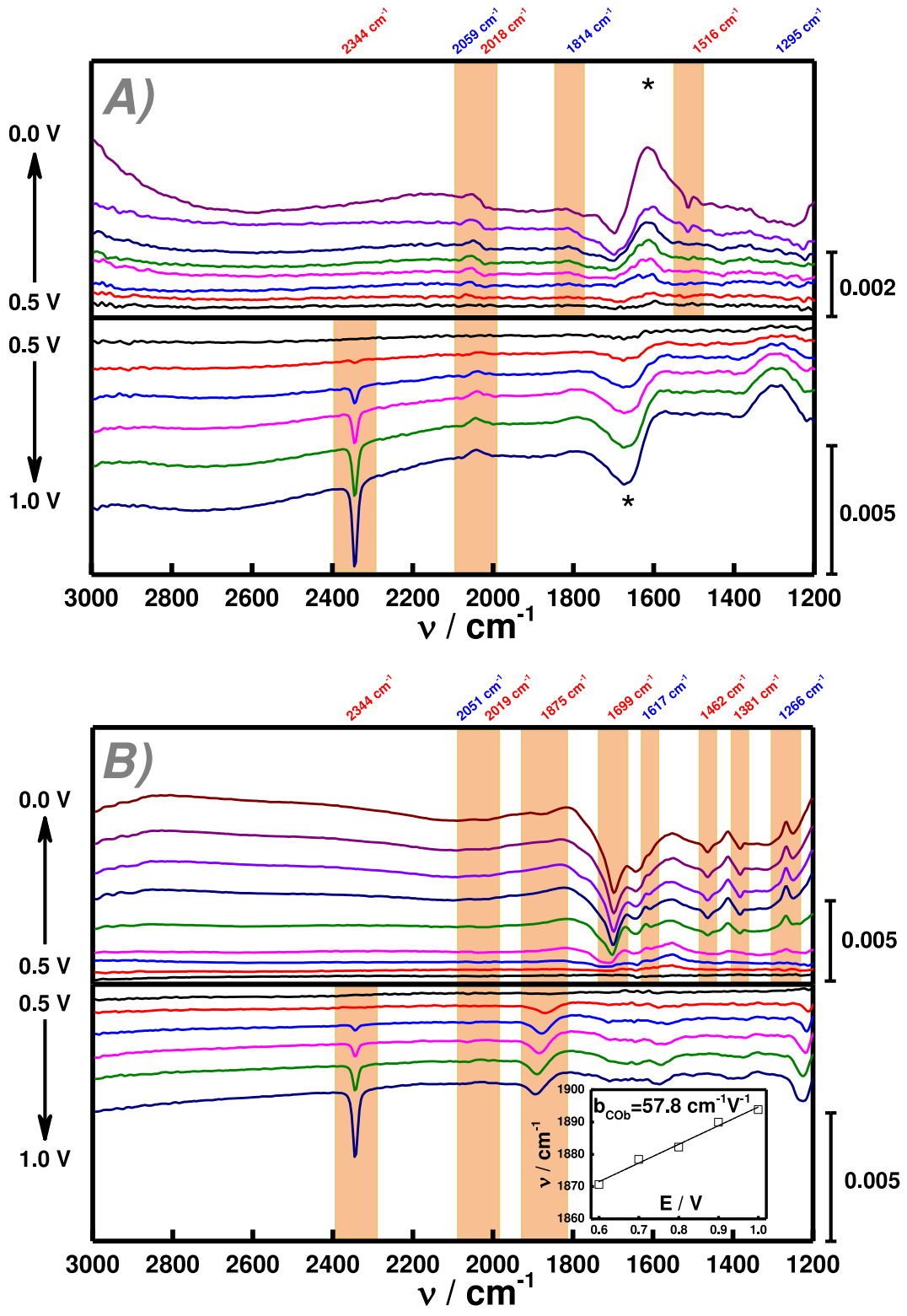

Fig. 3. FTIR spectra using p-polarized light of 10mM MVK in 0.1M sulfuric acid solution during the cathodic (upper panels) and subsequent anodic (lower panels) potential excursions on A) Pt(111) and B) PdML-Pt(111) electrodes. The reference spectrum was collected at E_{ads} = 0.5 V before each set of experiments. * is assigned to water bending band.

reduction is coupled to a solution-phase chemical reaction [24].

The electroactivity towards ECH of MVK can be almost fully recovered by expanding the potential window to 1.2 V and remains invariant when this anodic potential limit is included in every scan. After 10 cycles in the supporting electrolyte, the CV of the Pt(111) surface remains practically the same, whereas the CV of PdML electrode shows a partial dissolution of the film (data not shown). On Pt(111), when MVK is present in the solution, two oxidation waves at ca. 0.9 V and 1.1 V are observed (red and blue curves in Fig. 1B). When MVK is pre-adsorbed on the electrode and oxidation of the corresponding adsorbate is carried out

without MVK in solution (light blue curve in Fig. 1B), an oxidation wave at a much more positive potential of 1.25 V is observed. Hence, the oxidation waves below 1.1 V must correspond primarily to dissolved MVK. It is clear that during the oxidative scan a poisoning species is removed from the surface, most likely adsorbed CO. On PdML-Pt(111), one oxidation wave above 1.2 V is observed when MVK is pre-adsorbed on the electrode or dissolved in the solution. Therefore, the oxidative process includes mainly adsorbed species. After expanding anodic potential up to 1.4V, the Pt(111) was flamed annealed and the PdML redeposited, if applicable. The deactivation process on both surfaces immediately restarts by narrowing the potential window between 0.5 and 0.0 V.

The selectivity of the MVK hydrogenation was studied by carrying out bulk electrolysis for two hours at different potentials, while sampling the catholyte solution at regular time intervals. The overall Faraday Efficiency (FE) and the reagent consumption as function of potential are shown in Figure 2. The product distribution at each potential is displayed on Table S1 in the Supporting Information. An more negative potential boundary compared to the voltammetric studies was used only to confirm or rule out the hydrogenation of C=O moiety at extreme cathodic conditions.

The Pt(111) electrode reduces MVK to 2-butanone for all studied potentials. The FE passes through a maximum of 60% at 0.0 V and then decays for E≤-0.1V. The MVK consumed after the two hours of electrolysis increases monotonically with more negative potentials, suggesting that the lowering of the FE is due to concomitant hydrogen evolution.

The ECH products of MVK on PdML-Pt(111) electrode differ slightly from Pt(111): only the C=C bond is reduced above 0.0 V giving 2-butanone as the main product, whereas a very small percentage of 2-butanol and 3-buten-2-ol (ca. 0.1%) are observed for E ≤ -0.1 V (see Table S1 in the Supporting Information). Both the FE and reagent consumption follow the same trend as a function of the applied potential, again due to concomitant hydrogen evolution.

Figure 2 confirms that above 0 V the conversion on the PdML-Pt(111) is higher than on Pt(111), as expected from the CVs in Fig. 1. However, in general the consumption rates should be not compared too literally as the conditions of the experiments in Figs. 1 and 2 are very different.

In order to shed light on the identity of the poisoning species, *in situ* FTIR spectroscopy was performed. Figure 3 reports the spectra of MVK-containing solution on Pt(111) and PdML-Pt(111). Initially, the potential is stepped from 0.5 V (E_{ads}, potential chosen as the reference spectrum) down to 0.0 V in 0.1 V steps and subsequently stepped back to the initial potential and then further up to 1.0 V. Prior to switching the direction of the potential in the positive direction, a stabilization time is imposed at E_{ads}. The E_{ads} was chosen to avoid or minimize faradaic processes (the C=C dissociative adsorption occurs inevitably also for E ≤ 0.5V as evidenced later by a potential-opening experiment). The results are derived from p-polarized light. Only the spectral window between 1800 to 2400 cm^{-1} proved to be related to adsorbed species, as discerned by comparison with the spectra using s-polarized light (see Fig S3 in the Supporting Information).

On Pt(111) (Fig. 3A), one weak bimodal-type signal is observed at E ≤ 0.4V, with the positive and negative branch located at 2059 and 2018 cm^{-1}, respectively. This band can be assigned to the C-O stretching of CO adsorbed atop (CO_{atop}) as the frequencies agree with those reported in the literature [21]. The bimodal character indicates that the CO was adsorbed already at E_{ads}. A second faint bimodal-type band can be distinguished at 1814 cm^{-1} for E ≤ 0.3V and implies the existence of CO_{bridge} on the Pt(111) electrode [25]. When the potential is below 0.05 V, two weak negative-going bands centered at 1695 and 1516 cm^{-1} start growing, corresponding to a dissolved species, because they are also observed with s-polarized light (Fig. S3A). The band at 1695 cm^{-1} can be attributed to the carbonyl stretching from a saturated ketone, in this case, 2-butanone (see Fig S3 in the Supporting Information for references in aqueous media). Unfortunately, its detection is highly concealed by the water bending band at 1640 cm^{-1}. Since the band at 1516 cm^{-1} is absent in any of the expected MVK reduction by-products

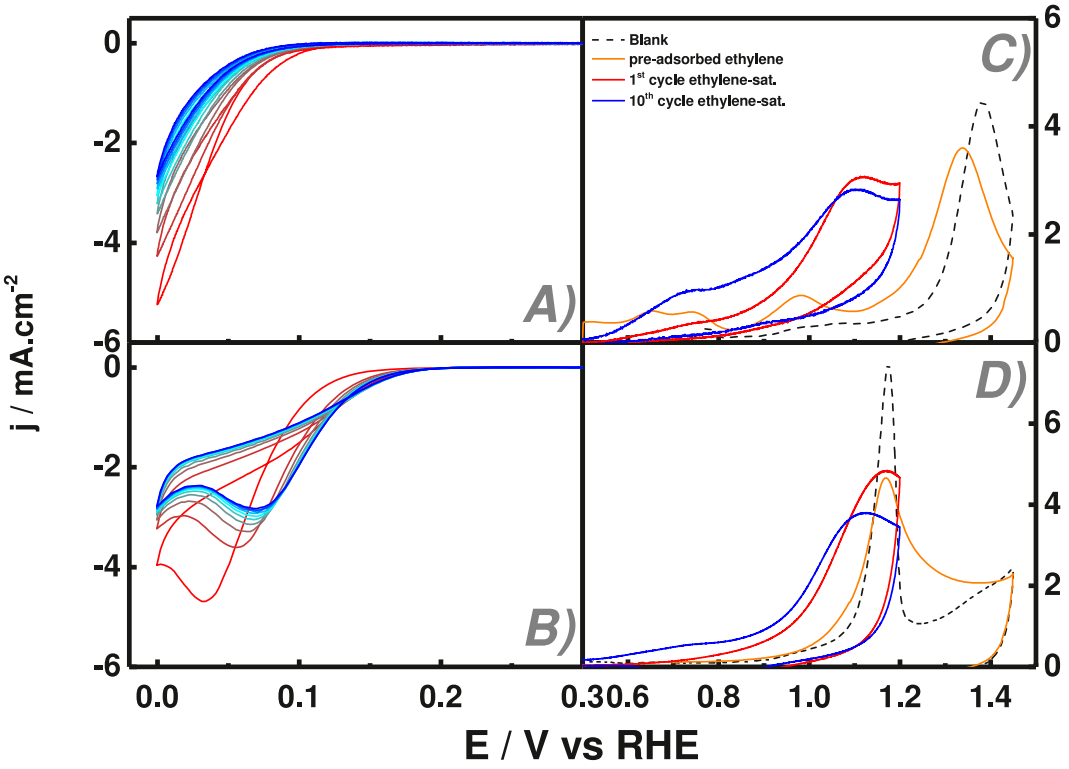

Fig. 4. Consecutive cyclic voltammetry of ethylene-saturated 0.1 M sulfuric acid solution for A) Pt(111) and B) PdML-Pt(111) electrodes at 50 mV s^{-1} starting from and ending at E_{ads}= 0.5 V. 1st and 10th cycle (red and blue lines, respectively) at 50 mV s^{-1} and anodic stripping at 10 mV s^{-1} of pre-adsorbed ethylene at E_{ads}= 0.5 V (light blue lines) for C) Pt(111) and D) PdML-Pt(111) electrodes. The blank CV for each surface is shown in black dashed lines.

(derivatives without carbon loss) listed in Fig. S4 and in possible soluble C-C breaking products resulting from the CO formation (such as acetone), its identity is not resolved.

When E ≥ 0.6, a strong negative band at 2345 cm^{-1} grows simultaneously with a positive band at 2044 cm^{-1}. The band at 2345 cm^{-1}, observed with both s- and p-polarized light, indicates the evolution of CO_2. The positive band at 2044 cm^{-1}, corresponding to the consumption of CO_{top}, evolves concomitantly and therefore they are likely connected.

On PdML-Pt(111) (Fig. 3B), three negative-going bands corresponding to $\nu_{C=O}$ (at 1697 cm^{-1}), a symmetric bend C=CH_2 (1460 cm^{-1}) and central ν_{C-C} (1380 cm^{-1}) [26], start growing when the potential is ≤ 0.2 V. All bands are also observed using s-polarized light, confirming that they belong to a dissolved species. All bands are present in the reference spectrum of 2-butanone (see Fig. S2) and therefore confirm its synthesis in the bulk at E_{onset}≈0.2V. Moreover, the ECH of the C=C is confirmed by two positive bands at 1617 ($\nu_{C=C}$) and 1266 cm^{-1} (assigned to the out-of-phase δ_{C-H} of the vinyl group). The more intense bands of 2-butanone observed on this surface compared to Pt(111) confirms that the rate of MVK reduction is slower on Pt(111).

When the potential is made more positive than E_{ads}, a negative and potential-dependent band at 1875 cm^{-1} is detected at E ≥ 0.6 V. This band corresponds to $\nu_{C=O}$ of CO_{bridge} corroborated by energies and Stark effect matching with the ones reported in the literature [25]. Its potential of oxidation agrees with the values reported for a Pd(111) single crystal under similar electrochemical conditions for low-to-medium coverage (ranging from 0.38 to 0.6) [27], and also with the first oxidation wave in the CV (see Fig. 1D). Furthermore, the corresponding Stark tuning slope (58 $cm^{-1}.V^{-1}$, see inset of Fig 3B) agrees with the values ranging from 42 to 50 $cm^{-1}.V^{-1}$ reported in the literature [28, 29]. For E ≥ 0.7 V, the FTIR spectrum shows the evolution of CO_2 (represented by narrow downward signal at 2344 cm^{-1}). However, no clear spectroscopic evidence of the CO_2 precursor is obtained and hence its origin remains elusive. Considering that CO_{bridge} band appears at a lower potential than CO_2 formation and its intensity does not decrease upon increasing the potential, it can be concluded that CO_2 is not only generated from CO but also from another adsorbate whose IR signals are masked by dissolved species.

Further mechanistic conclusions can be drawn from complementary studies on the reduction of the separate C=C and C=O functionalities. The electrochemical behavior of 3-buten-2-ol and 2-butanone on both surfaces is shown in Figure S5 in the Supporting information. First, similar reductive voltammetric behavior is found for 3-buten-2-ol (unsaturated alcohol) compared to MVK. The fact that the features in the cyclic voltammograms are analogous for the same electrode material in a solution containing either the α,β-unsaturated ketone or the α,β-unsaturated alcohol points to the reduction reaction of the same functional group, in this case, the vinyl moiety. The current decay upon cycling also suggests same deactivation process coming from the electroreduction of C=C bond. Secondly, 2-butanone absorbs very weakly (if at all) and cannot be reduced on atomically flat surfaces, as has been previously reported for the simplest ketone, e.g. acetone [12]. This is concluded from the cyclic voltammetry measurements on both Pt(111) and PdML-Pt(111), giving practically identical signals to their blanks in the same electrolyte solution (panels C and D, respectively).

The process of deactivation indicates an early and relatively extensive CO formation on Pt(111) whereas there is only limited CO formation on PdML-Pt(111). The poisoning occurs during the reduction of vinyl moiety in MVK. To confirm this conclusion, we decided to study the ECH of ethylene by electrochemical and spectro-electrochemical experiments, to see if the same effects occur with ethylene.

Figure 4 shows the cyclic voltammetry results for Pt(111) and PdML-Pt(111) electrodes in a solution saturated with ethylene (ca. 4.6 mM [30]) initially biased at 0.5 V. When the Pt(111) is polarized cathodically, the current starts flowing at 0.15 V during the first scan without becoming mass-transport limited, while in the positive-going scan a crossing point exists around 0.03 V. The intensity decreases with a progressive number of cycles, in a similar fashion to MVK and 3-buten-2-ol (Fig. 1A and S4); note that after the third cycle there is no longer a crossing point and after ten cycles the profile does not change substantially.

The electrochemical response of ethylene reduction on the PdML-Pt (111) electrode also shows similar features to the voltammetric measurements of MVK. During the first cycle, a reductive wave centered at 0.03 V is observed in the cathodic sweep. When the direction of the scan is reversed, current continues flowing and becomes even larger for a small potential window related to the presence of two crossing points. In the following cycles, the peak potential shifts progressively to more positive values whereas the current density decreases until a stable CV is obtained after ca. 10 scans. In the final CV, the peak potential and the maximum current density are equivalent to the CV in presence of MVK. Finally, as with MVK, the electrocatalytic current for the ECH of ethylene is fully recovered on both surfaces by going to oxidative potential values (1.2 V), resulting in constant CV features for a minimum of 10 cycles.

On both electrodes, a similar voltametric response is obtained in the presence of MVK and ethylene, which verifies the reduction of the vinyl group during ECH of MVK molecule and suggests that the poisoning process occurs in a similar manner for both molecules.

If a Koutecky-Levich analysis is applied to RDE data for ethylene reduction on PdML-Pt(111) electrode (see Fig. S6 in the Supporting Information), a diffusion coefficient of 4.48×10^{-6} cm^2 s^{-1} is obtained and, analogously to MVK, it is ca. one order of magnitude lower than the value reported in the literature (1.51×10^{-5} cm^2 s^{-1}) [31]. Therefore, we believe that the ECH mechanism of both reagents are similar and involve a coupled homogeneous reaction, possibly the protonation of the molecule.

The observed trace crossings may be ascribed to the formation of intermediates that are more reactive than the parent reagent [32], [33]. In the ECH of ethylene, this intermediate might be vinylidene and/or ethylidyne, relying on the experimental evidences for ethylene adsorption under electrochemical conditions [34], UHV dissociative adsorption of ethane [35] and ethylene [36] and DFT calculations of chemisorbed C_2H_x [37] on the Pt(111) surface. Furthermore, ethylene dissociative adsorption is not only specific for Pt as ethylidyne formation has also been detected on other substrates, e.g. Pd(111) [38] and Rh (111) [39].

Insights about the ethylene adsorbates are obtained again from the electro-oxidation of pre-adsorbed C_2H_4 at 0.5V. On Pt(111), four oxidative waves are observed. It is likely that the second wave (E = 0.74V) corresponds to the oxidation of CO residues as it coincides with the reported potential for its oxidative stripping [40]. The adsorbed CO must originate from the dissociative adsorption at the immersion potential. The third band (located at 1.3 V) matches with the onset potential for PtO_x formation. On the other hand, only one anodic wave centered at approximately 1.2 V is observed using a PdML-Pt(111) electrode, implicating simultaneous oxidation of organic adsorbates and partial oxidation of the Pd monolayer.

Integrating the anodic sweep between 0.5 and 1.45 V and subtracting the charge of the blank CV, total anodic charges equal to 360 and 230 μC cm^{-2} were calculated on Pt(111) and PdML-Pt(111), respectively. Assuming full oxidation to CO_2 (involving 12 electrons) then the surface excesses of ethylene would correspond to 3.1×10^{-10} mol cm^{-2} for Pt (111) and 2.0×10^{-10} mol cm^{-2} for PdML electrode (ca. 0.2-0.3 ML), which are quite close to the ones obtained for pre-adsorbed MVK. These values, particularly on Pt(111) surface, agree remarkably well with the maximum surface coverage reported for ethylene on Pt [41] and therefore suggests both molecules comprise 4 Pt atoms on (111) orientation.

In presence of dissolved ethylene, a similar oxidation profile is obtained as in MVK-containing solution. There are two anodic waves located at 0.74 and 1.1 V during the first oxidative sweep up to 1.2 V, while only the more positive wave remains for the 10^{th} cycle on the Pt

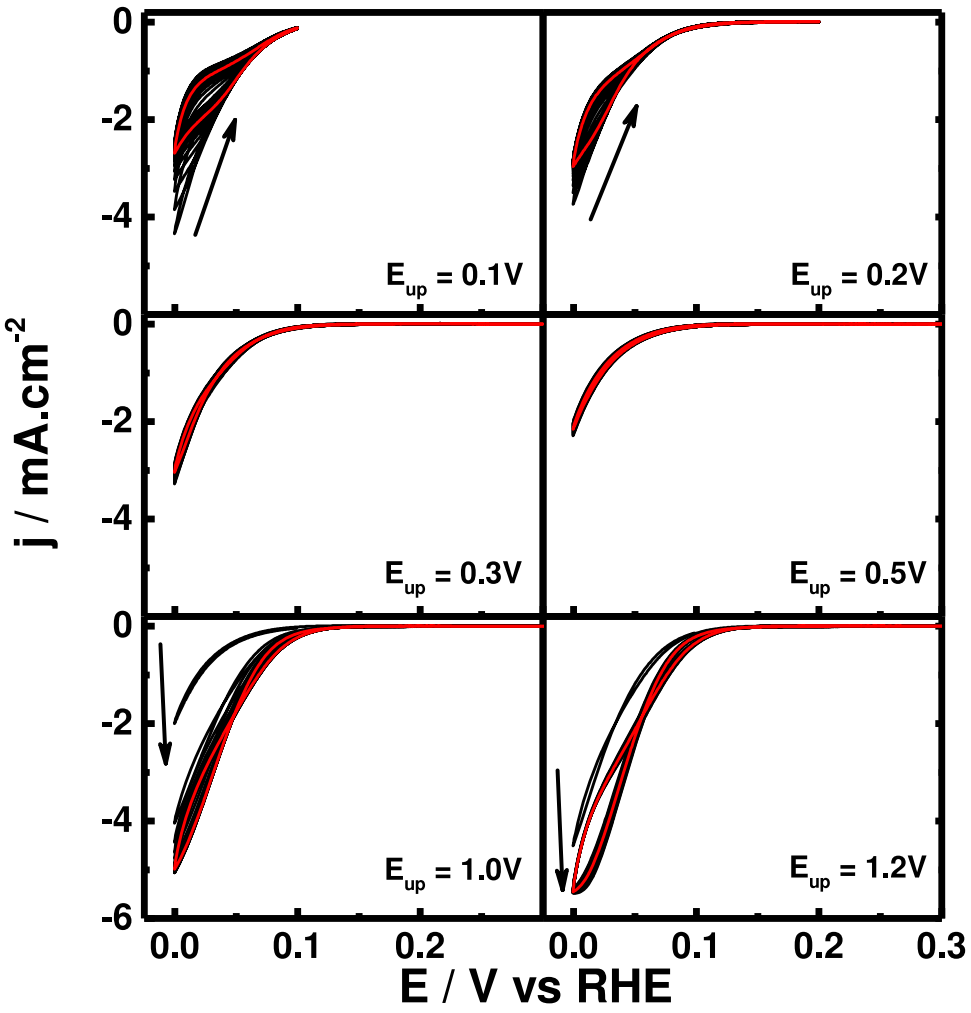

Fig. 5. Potential window-opening experiments in ethylene-saturated 0.1M sulfuric acid solution for Pt(111) electrode at 50 mV.s^{-1} starting from E_{ads}= 0.1 V. The red curve is the 10th cycle and the arrow shows the direction of the evolution.

(111) electrode. Along the same line, PdML-Pt(111) only gives one positive wave centered at 1.12 V. As we mentioned before for electro-oxidation of adsorbed ethylene, the absence of oxidation waves below 1.1 V indicates that CO poisoning does not happen to a significant extent on Pd.

To determine the potential at which deactivation starts, we started from a potential of 0.1 V where hydrogen is the dominant species on the surface and then scan it up to increasing upper vertex potential E_{up}. Figures 5 and 6 show these potential-opening experiments in ethylene-saturated solution for Pt(111) and PdML-Pt(111) electrodes, respectively.

In the narrowest potential range scanned (from 0.1 V to 0.0 V), the current on Pt(111) immediately starts flowing after the potential is being ramped negatively and evolves into a the plateau-like current right above 0.0 V with increasing number of cycles. The current density decreases continuously upon cycling, showing that the poisoning adsorbate is formed already at low potentials. With more positive E_{up}, the deactivation appears faster but it is limited and does not progress over time. Only if the E_{up} reaches the potential where the ethylene adsorbate is oxidized (1.0 V and higher), the ethylene reduction reactivates (see the CVs for E_{up} = 1.0 and 1.2 V).

On the PdML-Pt(111) electrode, the potential window-opening experiments reveal a different picture (Figure 6). Cycling between 0 and 0.1 V, a fairly constant negative current is measured, followed by an increase close to 0.0 V due to HER. The lack of progressive deactivation on PdML-Pt(111) suggests that a poisoning species is not formed in this potential range. Two cathodic peaks (labeled P_1 *and* P_2) start appearing when E_{up}= 0.2 V, which become more intense and shift slightly towards lower potentials upon expanding the potential window up to 1.0 V. For E_{up}= 1.2 V, only one broad cathodic peak (P_3) is observed, with a peak potential and current coinciding with the first scan of the CV initiated at E_{ads}=0.5V. Similar to MVK, a total recovery of electrocatalytic current is observed by expanding the potential window to very oxidative values (1.2 V).

Figure 7 depicts *in situ* FTIR spectra of ethylene-saturated solution in contact with Pt(111) or PdML-Pt(111) electrodes polarized at the labeled potentials. The potential sequence and the polarization of the light are identical to the ones used above for MVK. Experiments using s-polarized light were also performed for comparison (see Fig. S7 in the Supporting Information).

At potentials slightly lower than E_{ads}, the formation of CO_{top} is observed through a bimodal band (positive-going side centered at 2044-2050 cm^{-1} and a negative-going side centered at 2016-2023 cm^{-1}) on both surfaces, analogous to what was observed in MVK-containing solution (Fig. 3A and B). The generation of the same adsorbate in absence of carbonyl groups indicates that the CO comes from the dissociative adsorption of the C=C moiety [42]. However, the CO_{top} adsorbate is much more dominant on Pt(111), while the band intensity is much smaller on the PdML-coated electrode.

Other two IR features observed on both electrode materials are a weak negative-going band at 2885 cm^{-1}, appearing simultaneously with a weak bimodal band with positive and negative sides centered at 1442

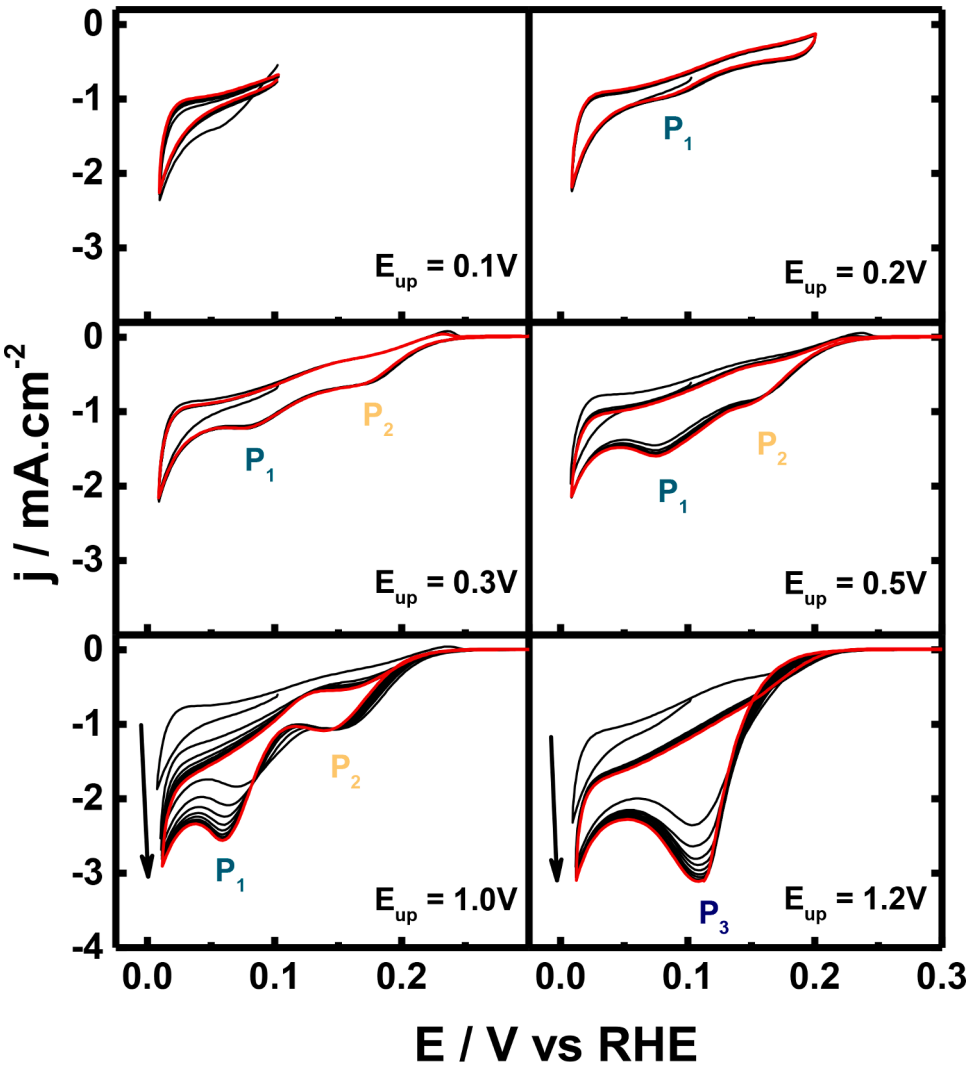

Fig. 6. Potential window-opening experiments in ethylene-saturated 0.1M sulfuric acid solution for PdML-Pt(111) electrode at 50 mV.s^{-1} starting from E_{ads}= 0.1 V. The red curve is the 10th cycle and the arrow shows the direction of the evolution.

and 1466 cm^{-1}, respectively. The onset potential for these bands are 0.15 and ca. 0.0V for the PdML-Pt(111) and Pt(111) electrode, respectively. These bands correspond to soluble species: a) alkyl compounds with a band above 2800 cm^{-1} belonging to C-H stretching, more intense for (C(sp^3)) than vinyl compounds (C(sp^2)) [43], and b) the bimodal band arises from the convolution of C-H scissoring bands from the ethane formed, leading to the negative feature at 1466 cm^{-1}, and the ethylene consumed, leading to the positive feature at 1442 cm^{-1}.

Below E_{ads}, the Pt(111) surface exposes a bimodal-type band at ca. 1625 cm^{-1}. This wavenumber lays in the spectral window of (μ-C=CH$_2$) [34,44] and might represent the formation of vinylidene adsorbates at the contact potential. Also, at potentials of ca. 0.1 V, a weak negative signal at 1336 cm^{-1} becomes visible. It is absent in spectra obtained with s-polarized light, which means that it corresponds to an adsorbate. Screening possible ethylene adsorbates, we found that ethylidyne species (≡C-CH$_3$) [45] has an IR active mode close to the wavenumber observed in our experiments, attributed to the symmetric (umbrella) mode of CH$_3$. Fragments of this adsorbate are predicted by DFT [38] to be formed at high hydrogen coverage and they should present another symmetric stretching mode at 2882-2886 cm^{-1}, which might be masked by ν_{CH3} mode of the ethane produced in the bulk of the solution. We can argue that these two bands are interconnected as their intensities change in opposite direction below E = 0.1 V, which indicates interconversion of μ-vinylidene into ethylidyne adsorbate. Furthermore, they do not disappear upon synthesis of ethane at ca. 0.0 V, meaning that these fragments act as spectators.

The ramp towards oxidative potentials also shows good agreement with the spectra compared to the electro-oxidation of MVK. CO_2 is quantitatively produced in the solution together with the consumption of adsorbed CO_{top} on both surfaces. Concomitantly, the vinylidene (1680 cm^{-1}) and ethylidyne (1337 cm^{-1}) adsorbates are also consumed on Pt(111), evidencing multiple CO_2 precursors. On PdML-Pt(111), two extra signals are observed between 0.7 and 1.0 V: a) a weak negative-going band at 1718 cm^{-1}, which can probably be assigned to an oxygenated carbon species (possibly carbonyl or carboxylate group [46]), and b) potential-dependent red-shifted band between 1830 and 1890 cm^{-1}, wavenumbers that match with $CO_{3\text{-fold}}$ [29]. The former species might be the second poisoning agent, difficult to observe during the ECH of MVK due to the total concealment by the carbonyl band.

Sulfate adsorption is also observed on Pt(111) by a negative-going band in the range of 1225-1270 cm^{-1} with a Stark slope value of 153 cm^{-1}/V, both in good agreement with reported values [47]. The process takes place simultaneously to the CO oxidation, from which we argue that CO impedes the anion adsorption. On PdML-Pt(111) it is more difficult to observe as the sulfate band is centered at 1220 cm^{-1}, as reported elsewhere [48], coinciding with the instrumental limit. However, part of the band starts to develop at ca. 0.15 V, which agrees with the potential of H/(bi)sulfate exchange on the electrode surface [22], while

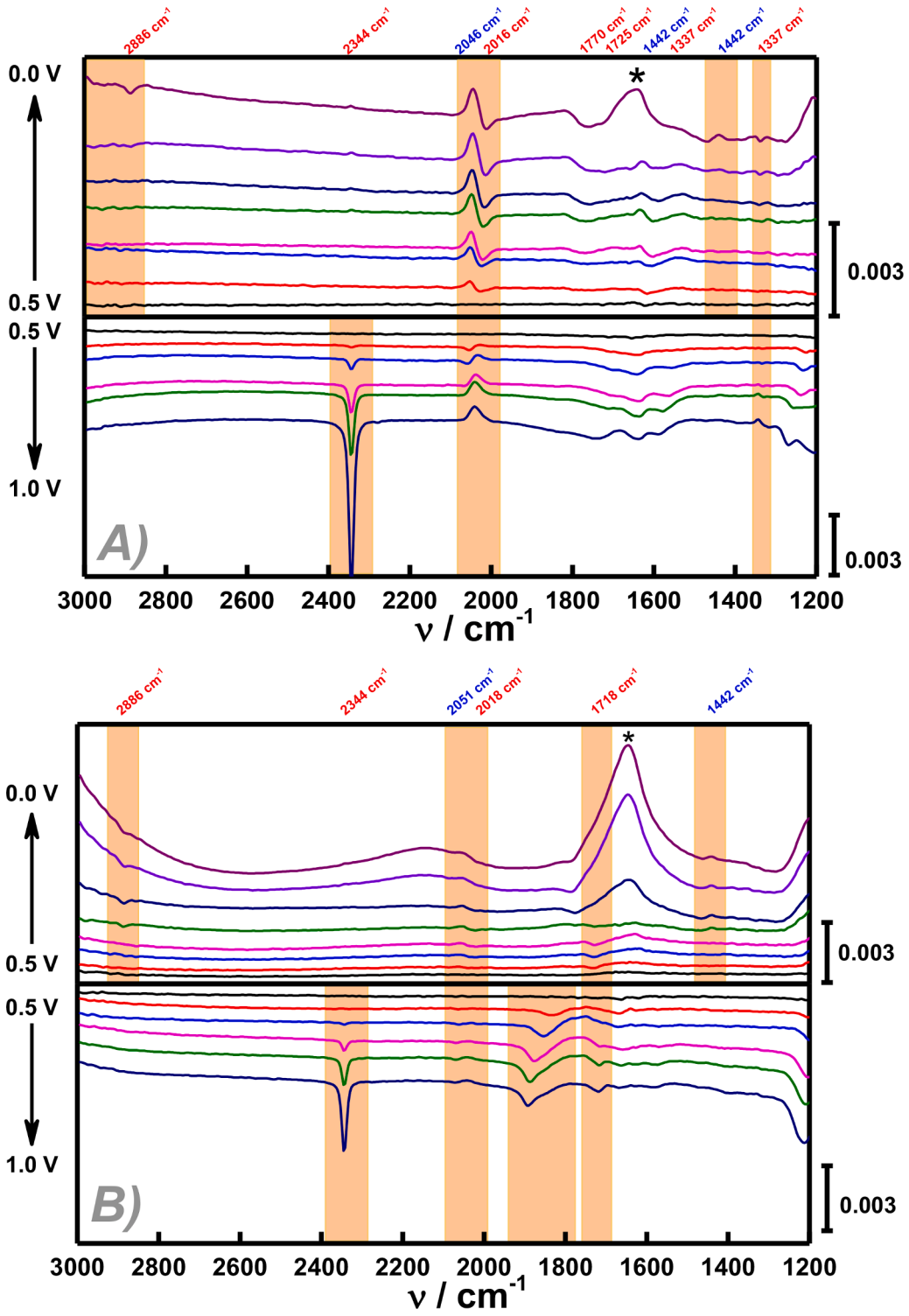

Fig. 7. FTIR spectra of ethylene-saturated electrolyte solution during the negative (upper panels) and subsequent positive potentials (lower panels) on A) Pt(111) and B) PdML-Pt(111) electrodes, using p-polarized light. The background was collected at E_{ads} = 0.5 V before acquiring each set of FTIR spectra. * is assigned to water bending band.

it changes direction above E = 0.7 V. The fact that sulfate can adsorb in almost the full potential window indicates that the surface is not blocked by organics or CO and further suggests that vinyl compounds adsorb weakly (or not at all) on PdML-Pt(111).

3.1. General discussion and conclusions

From the evaluation of the above results, we conclude that the hydrogenation of the vinyl moiety is preferred over the carbonyl group of the MVK molecule on both studied surfaces. This is confirmed by the almost identical electrochemical behavior during the hydrogenation of MVK and ethylene above 0.0 V vs. RHE on both surfaces. Ethane is the

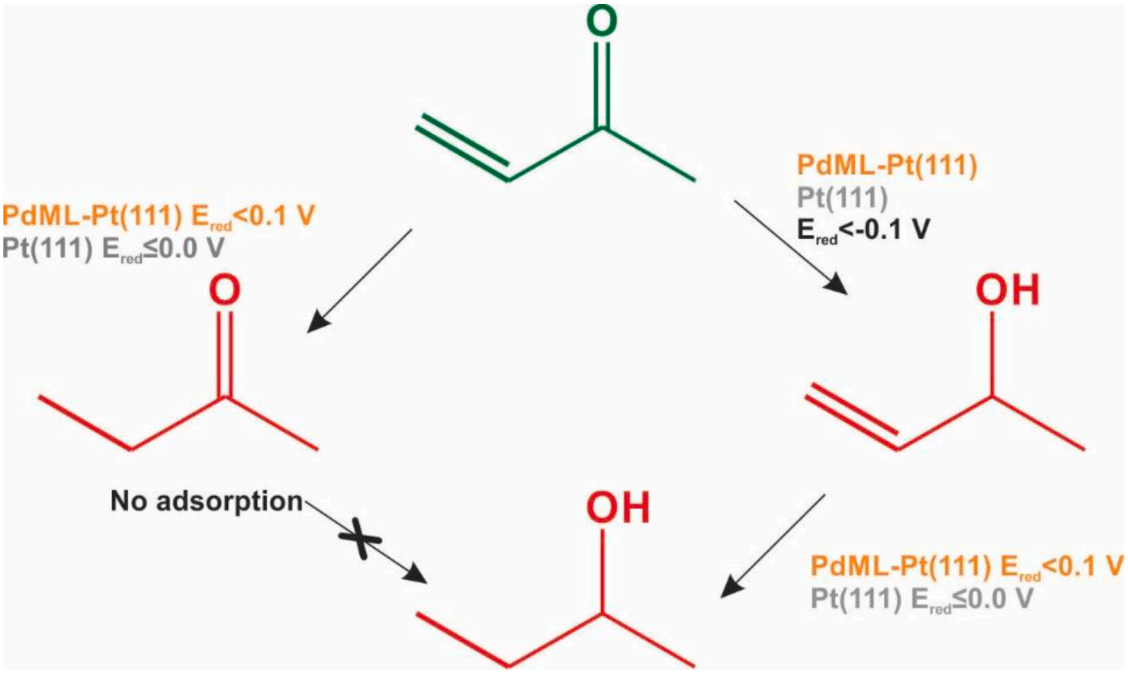

Scheme 1. Reaction pathways for MVK and its hydrogenation products on Pt(111) and PdML-Pt(111). The carbonyl function can be reduced at negative potentials only if the molecule can adsorb. The vinyl moiety (including ethylene) is hydrogenated in the H_{UPD} region. Production of 2-butanol at higher overpotentials than 3-buten-2-ol suggests that it is formed from 2-butenol, not from butanone.

only detectable product of ethylene ECH, and adsorbed CO is formed at the adsorption potential on Pt(111) to a much larger extent than on PdML-Pt(111). In parallel, the carbonyl moiety alone, as in 2-butanone, is not reduced on the studied surfaces within the H_{UPD} potential windows, as evidenced by the identical cyclic voltammograms in presence and absence of the saturated ketone. The lack of reactivity might be related to a weak interaction of the molecule with the surface of the catalysts under aqueous electrochemical conditions.

Below 0.0 V, the formation of small quantities of 2-butanol and 3-buten-2-ol from the reduction of MVK verifies the feasibility of the carbonyl group to be hydrogenated with an additional overpotential. On mercury electrodes, the C=C reduction is favored by ca. 400 mV vs. carbonyl reduction [49], depending on pH and the carbonyl group [50, 51]. Taking into account the lack of reactivity of the 2-butanone above 0.0V (no carbonyl reduction) and the low overpotential required for the electroreduction of the vinyl group in the 3-buten-2-ol (same potential as MVK and ethylene), the proposed reaction pathway for the formation of the saturated alcohol is most likely two sequential 2e-/2H+ reactions with 3-buten-2-ol acting as the intermediate. The proposed mechanism is summarized in Scheme 1.

On Pt(111), three different adsorbates (vinylidene, ethylidene and CO) are generated from the C=C moiety at E = 0.5 V, but they do not participate in the reaction, as it also has been reported by DFT [38]. These species block the adsorption of hydrogen for E > 0 V, coinciding with the potential windows of ECH inactivity, whereas the hydrogenation reaction commences concomitantly to the evolution of hydrogen. Conversely, the absence of vinylidene and ethylidene adsorbates on PdML-Pt(111) indicates no reactant dehydrogenation upon adsorption, which is in good agreement with the observations in heterogeneous catalysis [52], allowing the surface adsorption processes of the pristine electrode (H/sulfate exchange). Under these conditions, the ECH takes place at the H_{ads}-covered surface, concluded from the potential opening experiments, preceded by a chemical reaction in solution (as derived from the discrepancy in diffusion coefficients). The evidence points to the necessity of hydrogen co-adsorbed on both surfaces for the ECH reaction to proceed. However, more information about the nature of the adsorbed hydrogen is needed in order to fully explain the difference in activity between Pd and Pt substrates. Finally, the surface deactivating species on Pt(111) is CO_{atop}, whereas PdML-Pt(111) is more resistant to CO-poisoning (it only forms at E ≥ 0.7 V), keeping a significant activity with only a relatively small loss in current.

Credit Author Statement

Matias Villalba: Conceptualization, Methodology, Investigation, Writing - Original Draft

Marc T. M. Koper: Conceptualization, Writing - Review & Editing, Supervision, Funding acquisition

Declaration of Competing Interest

The authors declare that they have no known competing financial interests or personal relationships that could have appeared to influence the work reported in this paper.

Acknowledgments

This research received funding from the Netherlands Organization for Scientific Research (NWO) in the framework of the fund New Chemical Innovations, project 731.015.204 ELECTROGAS, with financial support of Akzo Nobel Chemicals, Shell Global Solutions, Magneto Special Anodes (an Evoqua Brand) and Elson Technologies.

Supplementary materials

Supplementary material associated with this article can be found, in the online version, at doi:10.1016/j.electacta.2022.140264.

References

[1] L. Zhang, M. Zhou, A. Wang, T. Zhang, Selective hydrogenation over supported metal catalysts: from nanoparticles to single atoms, Chem. Rev. 120 (2020) 683–733.

[2] N.P. Martínez, M. Isaacs, K.K. Nanda, Paired electrolysis for simultaneous generation of synthetic fuels and chemicals, New J. Chem. 44 (2020) 5617–5637.

[3] C. Mohr, P. Claus, Hydrogenation properties of supported nanosized gold particles, Sci. Prog. 84 (2001) 311–334.
[4] P. Mäki-Arvela, J. Hájek, T. Salmi, D.Y. Murzin, Chemoselective hydrogenation of carbonyl compounds over heterogeneous catalysts, Appl. Catal. A 292 (2005) 1–49.
[5] S. Tuokko, P.M. Pihko, K. Honkala, First principles calculations for hydrogenation of acrolein on pd and pt: chemoselectivity depends on steric effects on the surface, Angew Chem. 55 (2016) 1670–1674.
[6] T.B.L.W. Marinelli, S. Nabuurs, V. Ponec, Activity and selectivity in the reactions of substituted α,β-unsaturated aldehydes, J. Catal. 151 (1995) 431–438.
[7] F. Delbecq, P. Sautet, Competitive C=C and C=O adsorption of α,β-unsaturated aldehydes on pt and pd surfaces in relation with the selectivity of hydrogenation reactions: a theoretical approach, J. Catal. 152 (1995) 217–236.
[8] C.J. Kliewer, M. Bieri, G.A. Somorjai, Hydrogenation of the α,β-unsaturated aldehydes acrolein, crotonaldehyde, and prenal over Pt single crystals: a kinetic and sum-frequency generation vibrational spectroscopy study, J. Am. Chem. Soc. 131 (2009) 9958–9966.
[9] K.-H. Dostert, C.P. O'Brien, F. Mirabella, F. Ivars-Barceló, S. Attia, E. Spadafora, S. Schauermann, H.-J. Freund, Selective partial hydrogenation of acrolein on Pd: a mechanistic study, ACS Catalysis 7 (2017) 5523–5533.
[10] M.S. Ide, B. Hao, M. Neurock, R.J. Davis, Mechanistic insights on the hydrogenation of α,β-unsaturated ketones and aldehydes to unsaturated alcohols over metal catalysts, ACS Catalysis 2 (2012) 671–683.
[11] G.P. Sakellaropoulos, S.H. Langer, Electrocatalytic hydrogenation of ethylene over palladium at positive potentials, J. Catal. 67 (1981) 77–89.
[12] C.J. Bondue, F. Calle-Vallejo, M.C. Figueiredo, M.T.M. Koper, Structural principles to steer the selectivity of the electrocatalytic reduction of aliphatic ketones on platinum, Nature Catalysis 2 (2019) 243–250.
[13] T. Hartung, H. Baltruschat, Differential electrochemical mass spectrometry using smooth electrodes: adsorption and hydrogen/deuterium exchange reactions of benzene on platinum, Langmuir 6 (1990) 953–957.
[14] B. Bänsch, T. Härtung, H. Baltruschat, J. Heitbaum, Reduction and oxidation of adsorbed acetone at platinum electrodes studied by DEMS, J. Electroanal. Chem. Interfacial Electrochem. 259 (1989) 207–215.
[15] S.H. Langer, G.P. Sakellaropoulos, Kinetics of electrogenerative hydrogenation over platinum black electrocatalyst, J. Electrochem. Soc. 122 (1975) 1619–1626.
[16] H.G. Roth, N.A. Romero, D.A. Nicewicz, Experimental and calculated electrochemical potentials of common organic molecules for applications to single-electron redox chemistry, Synlett 27 (2016) 714–723.
[17] Z.J. Barton, G.H. Garrett, N. Kurtyka, T.D. Spivey, J.A. Schaidle, A. Holewinski, Electrochemical reduction selectivity of crotonaldehyde on copper, J. Appl. Electrochem. (2020).
[18] K. Shimazu, H. Kita, Hydrogenation of 1,3-butadiene on Pd in sulfuric acid solution: II. Adsorbed hydrogen species, J. Catal. 83 (1983) 407–414.
[19] O.A. Hazzazi, S.E. Huxter, R. Taylor, B. Palmer, L. Gilbert, G.A. Attard, Electrochemical studies of irreversibly adsorbed ethyl pyruvate on Pt{hkl} and epitaxial Pd/Pt{hkl} adlayers, J. Electroanal. Chem. 640 (2010) 8–16.
[20] H.-B. Ma, T. Sheng, W.-S. Yu, J.-Y. Ye, L.-Y. Wan, N. Tian, S.-G. Sun, Z.-Y. Zhou, High catalytic activity of Pt(100) for CH4 electrochemical conversion, ACS Catalysis 9 (2019) 10159–10165.
[21] J. Inukai, M. Ito, Electrodeposition processes of palladium and rhodium monolayers on Pt(111) and Pt(100) electrodes studied by IR reflection absorption spectroscopy, .l. Electroanal. Chem. 358 (1993) 307–315.
[22] X. Chen, L.P. Granda-Marulanda, I.T. McCrum, M.T.M. Koper, Adsorption processes on a Pd monolayer-modified Pt(111) electrode, Chem. Sci. 11 (2020) 1703–1713.
[23] Chemical properties for calculation of impact to ground water soil remediation standards, 2008.
[24] S. Rebouillat, M.E.G. Lyons, T. Bannon, Evaluation of the proton transfer kinetics of potential electrolytes in non-aqueous solutions using electrochemical techniques Part 1. Kinetic analysis of the general CE mechanism at stationary and rotating electrodes, J. Solid State Electrochem. 3 (1999) 215–230.
[25] B.E. Heyden, A.M. Bradshaw, The adsorption of CO on Pt(111) studied by infrared reflection—Absortion spectroscopy, Surf. Sci. 125 (1983) 787–802.
[26] R. Lindenmaier, S.D. Williams, R.L. Sams, T.J. Johnson, Quantitative infrared absorption spectra and vibrational assignments of crotonaldehyde and methyl vinyl ketone using gas-phase mid-infrared, far-infrared, and liquid raman spectra: s-cis vs s-trans composition confirmed via temperature studies and ab initio methods, J. Phys. Chem. A 121 (2017) 1195–1212.
[27] Y. Kenjiro, K. Fusao, T. Mitsuaki, T. Machiko, I. Masatoki, Infrared reflection absorption spectra of carbon monoxide adsorbed on single crystal electrodes, Pd (111) and Pd(100), Surf. Sci. 227 (1990) 90–96.
[28] M.C. Figueiredo, D. Hiltrop, R. Sundararaman, K.A. Schwarz, M.T.M. Koper, Absence of diffuse double layer effect on the vibrational properties and oxidation of chemisorbed carbon monoxide on a Pt(111) electrode, Electrochim. Acta 281 (2018) 127–132.
[29] S.-C. Chang, M.J. Weaver, Coverage- and potential-dependent binding geometries of carbon monoxide at ordered low-index platinum- and rhodium-aqueous interfaces: comparisons with adsorption in corresponding metal-vacuum environments, Surf. Sci. 238 (1990) 142–162.
[30] E.J. Bradbury, D. McNulty, R.L. Savage, E.E. McSweeney, Solubility of Ethvlene in Water: effect of the temperature and pressure, Ind. Eng. Chem. 44 (1952) 211–212.
[31] A. Huq, T. Wood, Diffusion coefficient of ethylene gas in water, J. Chem. Eng. Data 13 (1968) 256–259.
[32] Y.X.C. Goh, H.M. Tang, W.L.J. Loke, W.Y. Fan, Bis(cyclopentadienyl)nickel(II) mu-thiolato complexes as proton reduction electrocatalysts, Inorg. Chem. 58 (2019) 12178–12183.
[33] C. Amatore, J. Pinson, J.M. Savéant, A. Thiebault, Trace crossings in cyclic voltammetry and electrochemic electrochemical inducement of chemical reactions: Aromatic nucleophilic substitution, J. Electroanal. Chem. Interfacial Electrochem. 107 (1980) 59–74.
[34] A. Berná, A. Kuzume, E. Herrero, J.M. Feliu, Ethylene adsorption and oxidation on Pt(hkl) in acidic media, Surf. Sci. 602 (2008) 84–94.
[35] J.J.W. Harris, V. Fiorin, C.T. Campbell, D.A. King, Surface products and coverage dependence of dissociative ethane adsorption on Pt{110}-(1 × 2), J. Phys. Chem. B 109 (2005) 4069–4075.
[36] T.A. Land, T. Michely, R.J. Behm, J.C. Hemminger, G. Comsa, STM investigation of the adsorption and temperature dependent reactions of ethylene on Pt(111), Appl. Phys. A 53 (1991) 414–417.
[37] J. Kua, W.A. Goddard, Chemisorption of Organics on Platinum. 2. Chemisorption of C2Hx and CHx on Pt(111), J. Phys. Chem. B 102 (1998) 9492–9500.
[38] L.V. Moskaleva, Z.-X. Chen, H.A. Aleksandrov, A.B. Mohammed, Q. Sun, N. Rösch, Ethylene conversion to ethylidyne over Pd(111): revisiting the mechanism with first-principles calculations, J. Phys. Chem. C 113 (2009) 2512–2520.
[39] M. Li, W. Guo, R. Jiang, L. Zhao, X. Lu, H. Zhu, D. Fu, H. Shan, Mechanism of the ethylene conversion to ethylidyne on Rh(111): a density functional investigation, J. Phys. Chem. C 114 (2010) 8440–8448.
[40] J.M. Orts, A. Fernández-Vega, J.M. Feliu, A. Aldaz, J. Clavilier, Electrochemical behaviour of CO layers formed by solution dosing at open circuit on Pt(111). Voltammetric determination of CO coverages at full hydrogen adsorption blocking in various acid media, J. Electroanal. Chem. 327 (1992) 261–278.
[41] E. Gileadi, B.T. Rubin, J.O.M. Bockris, Electrosorption of Ethylene on Platinum as a Function of Potential, Concentration, and Temperature, J. Phys. Chem. 69 (1965) 3335–3345.
[42] U. Schmiemann, U. Müller, H. Baltruschat, The influence of the surface structure on the adsorption of ethene, ethanol and cyclohexene as studied by DEMS, Electrochim. Acta 40 (1995) 99–107.
[43] H.L. McMurry, V. Thornton, The infrared spectra of propane and its symmetrical deuterium substituted analogs, J. Chem. Phys. 19 (1951) 1014–1018.
[44] D. Moigno, W. Kiefer, J. Gil-Rubio, H. Werner, Vibrational spectroscopy studies and density functional theory calculations on square-planar vinylidene, carbonyl and ethylene rhodium(I) complexes, J. Organomet. Chem. 612 (2000) 125–132.
[45] J.D. Krooswyk, C.M. Kruppe, M. Trenary, In-situ spectroscopic monitoring of the ambient pressure hydrogenation of C2 to ethane on Pt, Surf. Sci. 652 (111) (2016) 142–147.
[46] E.A. Monyoncho, S.N. Steinmann, C. Michel, E.A. Baranova, T.K. Woo, P. Sautet, Ethanol electro-oxidation on palladium revisited using polarization modulation infrared reflection absorption spectroscopy (PM-IRRAS) and density functional theory (dft): why is it difficult to break the C–C Bond? ACS Catalysis 6 (2016) 4894–4906.
[47] T. Wandlowski, K. Ataka, S. Pronkin, D. Diesing, Surface enhanced infrared spectroscopy—Au(111-20nm)/sulphuric acid—new aspects and challenges, Electrochim. Acta 49 (2004) 1233–1247.
[48] B. Alvarez, V. Climent, A. Rodes, J.M. Feliu, Anion adsorption on Pd–Pt(111) electrodes in sulphuric acid solution, J. Electroanal. Chem. 497 (2001) 125–138.
[49] P. Tömpe, G. Clementis, I. Petneházy, Z.M. Jászay, L. Tőke, Quantitative structure-electrochemistry relationships of α, β-unsaturated ketones, Anal. Chim. Acta 305 (1995) 295–303.
[50] D. Barnes, P. Zuma, Polarographic reduction of aldehydes and ketones part VI.-Behaviour of cinnamaldehyde at lower pH-values, Trans. Faraday Soc. 65 (1968) 1668–1680.
[51] L. Spritzer, P. Zuman, Polarographic reduction of aldehydes and ketones: Part XXII. Reduction and oxidation of α,β-unsaturated aldehydes: Acrolein, tiglaldehyde and substituted cinnamaldehydes, J. Electroanal. Chem. Interfacial Electrochem. 126 (1981) 21–53.
[52] D. Stacchiola, S. Azad, L. Burkholder, W.T. Tysoe, An investigation of the reaction pathway for ethylene hydrogenation on Pd(111), J. Phys. Chem. B 105 (2001) 11233–11239.